

Enhancement of CD4⁺CD25⁺ T cells in tumor growth of benzo[a]pyrene-induced forestomach carcinoma via suppression of local immunity

Yi-Ling Chen¹, Jung-Hua Fang², Ming-Derg Lai⁴, Chia-Jui Yen³, Yan-Shen Shan²

¹Department of Childhood Education and Nursery, Chia-Nan University of Pharmacy and Science, Tainan, Taiwan

² Division of Surgery, Department of Surgery, ³ Division of Hemato-oncology, Department of Internal Medicine, National Cheng Kung University Hospital, ⁴Department of Biochemistry and Molecular Biology, College of Medicine, National Cheng Kung University, Tainan, Taiwan

Correspondence: Yan-Shen Shan, MD PhD
Assistant Professor

Division of Surgery, Department of Surgery, National Cheng Kung University Hospital, College of Medicine, National Cheng Kung University, Tainan, Taiwan.

138, Sheng-Li Road, Tainan 70428, Taiwan (ROC)

Tel: 886-6-2353535, ext 5181

Fax: 886-6-2766676

e-mail: ysshshan@mail.ncku.edu.tw

***Key words:* CD4⁺CD25⁺ regulatory T cells, forestomach tumor, Foxp3, lymph node**

Abbreviations used in this paper: Treg, regulatory T; B[a]P, benzo[a]pyrene; TIL, tumour-infiltrating lymphocytes.

Abstract

The increased populations of Treg cells in peripheral blood and gastric carcinoma reflect compromised host immunity. **It remains unclear, whether the Treg cells in the lymphoid tissues contribute to the immune dysfunction in gastric cancer.** In this study, the murine model of benzo[a]pyrene(B[a]P)-induced forestomach carcinoma was used to analyze the distribution of Treg cell populations in different lymphoid tissues. To determine the enhancement of Treg cells on tumor growth, the Treg cells were depleted by PC61 specific antibody. The proportions of Treg cells in the thymus, spleen, the regional lymph nodes (nodes at the perigastric area and the mesentery, RLNs), and the peripheral lymph nodes (nodes at the axillary, inguinal, brachial, and popliteal, PLNs), were compared. The proportion of Treg cells in total CD4⁺ T cells is clearly increased in RLNs compared with PLNs, spleen and thymus in B[a]P-treated mice as tumor grown. Moreover, these cells express the Foxp3 transcript and were dramatically enhanced in RLNs relative to PLNs at 32 weeks. After depletion, the proportion of Treg cells decreased in the lymphoid tissues, especial in the RLNs, the tumor mass reduced significantly, and massive infiltrating cells at the tumor sites and apoptosis of the tumor masses were observed in the forestomach carcinomas of the B[a]p treated mice at 32 weeks. These results demonstrate that the accumulation of Treg cells in the regional lymph nodes mediated suppressive immunity in progressive forestomach tumors. Treg cells depletion reduces growth of tumor via effective local immunity.

Introduction

Regulatory T (Treg) cells, activated CD4⁺ T cells that express CD25 (IL-2 receptor α chain), constitute 5~10% of peripheral CD4⁺ T cells in mice and humans (1-4). These Treg cells seem to play a pivotal role in immune homeostasis, protecting the host from T-cell-mediated autoimmune disorders including type 1 diabetes, hypothyroidism, pernicious anemia and inflammatory colitis. The immune regulatory function of these Treg cells has been attributed to their capacity to secrete immunosuppressive cytokines, including IL-10 and TGF- β 1 (5). Although beneficial to protect host from autoimmune disease, Treg cells may also dampen antitumor response. Evidence from various cancers demonstrates that the proportion of Treg cells increases in tumour-infiltrating lymphocytes (TIL) and peripheral circulation of gastric cancers (6-8), in the peripheral blood of patients with ovarian and lung cancers, hepatocellular carcinoma, and pancreas/breast adenocarcinoma (9-14). Local accumulation of Treg cells in tumors is associated with a high death hazard and reduced survival in ovarian carcinoma (10). These reports suggest that the Treg cells participate in cancer immunopathogenesis and are responsible for impairment of host immune surveillance to cancer. Viguier et al reported higher accumulation of Treg in metastatic melanoma lymph nodes in humans, and further demonstrated that these cells inhibited proliferation and cytokine production of infiltrating CD4⁺CD25⁻ and CD8⁺ T cells *in vitro* (15). In contrast, Curiel et al reported that Treg cells accumulated in ovarian tumors and malignant ascites, but not in draining lymph nodes in later cancer stages (10). Hence, it is necessary to elucidate the distributions and effects of Treg cells in local lymphoid tissues during progression of cancers.

The preserved, smoked, cured, and salted foods are highly associated with development of gastric cancer. PAHs are groups of carcinogens and are detected in cigarette smoke, in broiled and smoked foods (16). Among PAHs, benzo[a]pyrene (B[a]P) is the most studied compound, and induces many carcinogen-specific effects (17). After delivered by gavage, B[a]p-induced forestomach tumor is a common mouse model for study of chemopreventive

effect of substances of gastric cancer (18-21). To understand the immunosurveillance of Treg cells, B[a]P-induced forestomach tumor was used to evaluate the effect of Treg cells by intervention at the initiation, promotion, or progression stage of multistage carcinogenesis. Recently, depletion of CD25 can induce immune responses to variety of different tumors in mice including myeloma, leukemia, melanoma and fibrosarcoma (22-24). Lymphoid metastasis is also the determinative for gastric cancer. Therefore, first, we used the B[a]P-induced autochthonous forestomach tumor in female mice to analyze the distribution of T cell population in different lymphoid tissues during tumor progression. Secondly, to determine Treg cells were required for controlling tumor formation, mice were depleted of Treg cells by specific antibody.

Materials and Methods

Reagents and antibodies

Benzo[a]pyrene, glycerol gelatin, and propidium iodide (PI) were purchased from Sigma-Aldrich (St. Louis, MO). An aminoethyl carbazole substrate kit was purchased from Zymed (San Francisco, CA). Ficoll-paque was purchased from Amersham Biosciences (Uppsala, Sweden). The following Abs were purchased from BD PharMingen (San Diego, CA) and used in this study: rat IgG Ab (ICN Pharmaceuticals, Cappel, OH); mouse anti-CD4 PE (H129.19), anti-CD8a PE (53-6.7), anti-CD3e PE (145-2C11) and anti-CD25 FITC (7D4). Human anti-CD4 FITC and anti-CD25 PE were purchased from Immunotech (Marseille Cedex).

B[a]P -induced forestomach tumorigenesis

B[a]P-induced forestomach tumors were generated in female mice as previously reported (25). Eight-week-old ICR mice were purchased from the Laboratory Animal Center of National Cheng Kung University. All animal experiments were carried out with approval of the ethical committee of our institution. Benzo[a]pyrene was dissolved in corn oil. Control

and benzo[a]pyrene-treated mice received 200 μ l of corn oil with or without 3 mg of benzo[a]pyrene, respectively, by p.o. gavage twice weekly for 4 weeks. The mice were then sacrificed at week 7, 16 and 32 after the first administration of benzo[a]pyrene. Buffered formalin-phosphate (10%) was immediately injected into the stomach by oral intubation, so that the stomach was distended and fixed. Each stomach was then removed and placed on a plastic sheet, and the tumor incidence, number and volume in each forestomach was counted. All stomachs were assessed under dissecting microscopy, and tumor size was measured. Tumor volume was calculated using the formula: $\text{volume} = 4\pi R^3/3$ (26). The stomach samples were surgically obtained and immersed in a buffered 10% formalin solution for paraffin block preparation. Four-micrometer sections were dehydrated, embedded, and stained with hematoxylin and eosin.

***In vivo* regulatory T cell depletion**

CD25⁺ T cell-specific antibodies were produced using hybridoma PC61 from Dr. Lai MD Lab. To deplete the CD25⁺ T cells, mice were injected i.p. with 200 μ l ascitic fluid from PC61 mAb, a final concentration of 3 mg protein per ml (27) twice a week beginning 5 weeks after the B[a]P treatment. Control mice received the same treatment of purified rat IgG antibody. To evaluate the effectiveness of the depletion, splenocytes, thymocytes or lymphocytes from the peripheral lymph nodes were incubated with anti-CD4-PE (H129.19), anti-CD8 PE (53-6.7) and anti-CD25-FITC (7D4) at 4 $^{\circ}$ C for 40 min in the dark. The mixture was washed twice with ice-cold HBSS, and the cells resuspended in HBSS containing 2% FCS/0.1% NaN₃. Stained splenocytes, thymocytes or lymphocytes were analyzed by flow cytometry (FACS Calibur; BD Biosciences, San Jose, CA). The depressed number of CD4⁺CD25⁺ T cells in thymus, spleen and PLNs in naive mice was confirmed on the third and seventh days every week. Flow cytometry analyses of the CD25⁺ T cells post depletion revealed that they constituted numbers were less than 1%.

Cell preparations, sorting and flow cytometry analysis

Lymph nodes from the mice were collected on weeks 7, 16 and 32 after the first administration of B[a]P. The lymph nodes around the stomach and in the mesentery were collected and defined as regional lymph nodes (RLNs). The lymph nodes in the axillary, inguinal, brachial, and popliteal areas were collected and defined as peripheral lymph nodes (PLNs). Cell suspensions from the lymph nodes, thymus or spleen were isolated after sterile dissociation, filtration and washing. For isolation of CD4⁺CD25⁺ and CD4⁺CD25⁻ cells, RLNs, PLNs and the thymus were further separated by flow sorting. Cells were stained using PE-conjugated anti-CD4 and FITC-conjugated anti-CD25 and then purified on a FACS Aria sorting flow cytometer (BD Biosciences, San Jose, CA). The purity of these population of CD4⁺CD25⁺ and CD4⁺CD25⁻ T cells was >90%. To determine the expression of cell surface marker in T cells from RLNs, PLNs, thymus and spleen, the cells were incubated with antibodies appropriately diluted for staining. Stained lymphocytes were analyzed by flow cytometry.

Detection of apoptotic cells

Apoptotic cells in tumor nodules from stomach tissues were detected by TUNEL labelling detection of free 3'-OH groups in fragmented DNA in situ (Apop Tag-peroxidase in situ apoptosis detection kit, Chemicon). Paraffin-embedded, slide-mounted tissue sections were deparaffinized, and treated with proteinase K for 15 min followed by 3% H₂O₂ for 5 min at room temperature. After nick end labelling with digoxigenin-deoxyuridine triphosphate by terminal deoxynucleotidyl transferase, immunostaining was performed using peroxidase-conjugated anti-digoxigenin Ab. Apoptotic cells were visualized with diaminobenzidine substrate, becoming a dark-brown color. Specimens were then counterstained with haematoxylin.

Semi-quantitative and real-time PCR

Total RNA was extracted from 5×10⁵ sorted cells and purified using the RNeasy Kit according to the manufacturer's instructions (Qiagen, Valencia, CA) and converted to cDNA

by Moloney Murine Leukemia Virus (M-MLV) reverse transcriptase with oligo(dT) primer in the presence of RNAsin (Promega, Madison, WI). Semi-quantitative PCR for Foxp3, TGF- β , IL-10 and β -actin was performed as described previously (28, 29-31). The cDNA generated was subjected to 30-35 cycles of PCR amplification on a DNA Thermal Cycler (Perkin Elmer, GeneAmp PCR System). The β -actin served as a quantitative control for PCR. PCR products were fractionated by agarose gel electrophoresis, stained with ethidium bromide, and visualized under UV light.

Real-time PCR was performed on a LightCycler detection system (Roche Applied Science). Analyses were performed using primers, an internal fluorescent TaqMan Probe specific to Foxp3 or HPRT, and the LightCycler TaqMan Master kit (Roche Applied Science, Penzberg, Germany). The primer and TaqMan probe sequences were as follows as previously described (28). *Foxp3* primers: 5'-CCC AGG AAA GAC AGC AAC CTT-3' and 5'-TTC TCA CAA CCA GGC CAC TTG-3'; *Foxp3* probe: 5'-FAM-ATC CTA CCC ACT GCT GGC AAA TGG AGT C-3'; HPRT primers: 5'-TGA AGA GCT ACT GTA ATG ATC AGT CAA C-3' and 5'-AGC AAG CTT GCA ACC TTA ACC A-3'; HPRT probe: 5'-FAM-TGC TTT CCC TGG TTA AGC AGT ACA GCC C-3'. Standard curves of cDNAs from ICR mice CD4⁺CD25⁺ T cells were used as previously described (28). The normalized values for Foxp3 mRNA were calculated as the relative quantity of Foxp3 mRNA levels divided by the relative quantity of HPRT mRNA levels. All samples were run in triplicate.

Lymphocyte preparation and flow cytometry analysis from N1 regional lymph in patients with gastric cancer

Twenty milliliters of heparinized peripheral blood was obtained from patients with gastric cancer. PBMCs were isolated with Ficoll-paque density gradient. Tumor, normal gastric mucosa (5cm away from tumor), and N1 regional lymph nodes in the stomach of patients with gastric cancer were collected during surgery. The infiltrated lymphocytes of tumor and normal mucosa and lymph node cells suspensions were obtained after sterile

mechanical dissociation, then filtered and washed. A single-cell suspension was stained by FITC-conjugated anti-CD4 and PE-conjugated anti-CD25 mAb. Stained lymphocytes were analyzed by flow cytometry.

Statistical analysis

Results are expressed as mean \pm standard error or mean deviation. Values were compared using the student's t-test for independent experiments. A value of $P \leq 0.05$ was considered statistically significant.

Results

Histological analysis of benzo[a]pyrene-induced forestomach tumors in mice at 16 and 32 weeks

Mice were given corn oil or benzo[a]pyrene (B[a]P) by gavage twice weekly for 4 weeks. After the first dose of B[a]P, there was significant small rash-like tumor nodules formation in the forestomachs of the B[a]P-treated mice at 16 weeks, but no tumor growth was detected in the forestomachs of the corn oil-treated mice (Fig. 1A). The progressive processes of tumor formation were more evident at 32 weeks, with clear invasion of the fundic stomach by malignant cell carcinoma (Fig. 1A). Tumor incidence was 100% in the B[a]P-induced forestomachs of the animals at 16 and 32 weeks (Table 1). The number of detected tumor nodules increased during this period. Further, the tumor nodules in the B[a]P-treated mice were observed with typical pathological alternations. In addition, the numbers of papilloma and squamous cell carcinomas were both increased (Fig. 1B).

To determine whether immune cells infiltrated the tumor area, the histology of the stomachs was examined. We observed few granulocytes and lymphocytes accumulated in and around the tumor nodes from forestomach cancer in the B[a]P-treated mice at 16 and 32 weeks (Fig. 1B).

Treg depletion reduces growth of tumor nodules in B[a]P-treated mice

In preliminary studies, the murine model of B[a]P-induced forestomach tumors in female animals was used to analyze the distribution of the T cell population at 36 weeks. The lymph nodules of the B[a]P-treated mice had a significantly higher proportion of CD4⁺CD25⁺ T cells in total CD4⁺ T cells compared to the corn oil-treated animals (unpublished data). To determine whether CD25⁺ T cells were critical for enhancement of tumor formation, antibody (PC61) treatments was used to deplete CD25⁺ T cells. Depletion of CD4⁺CD25⁺ T cells was confirmed in the PLN, spleen and thymus of naïve ICR mice (Fig. 2A), with <1% diminution observed in these organs (Fig. 2B). We examined that naïve mice treated with PC61 antibody did not develop histologically evident autoimmunity (unpublished data). Then, to deplete the CD25⁺ T cells, mice were injected i.p. with the same dosage of ascitic fluid from PC61 mAb twice a week beginning 5 weeks after the B[a]P treatment. In the B[a]P-treated and CD25-depleted mice, forestomach tumor growth was progressively reduced after 16 and 32 weeks (Fig. 1A; Table 1). The B[a]P-treated and CD25-depleted mice significantly reduced 80% total tumor volume per mouse in comparison with B[a]P/IgG-treated mice at 16 weeks and 32 weeks, respectively (Table 1). Histological changes were observed at the tumor sites in B[a]P-treated and CD25-depleted mice, with analysis of the tumor nodules revealing a significant increase in granulocytes and lymphocytes infiltration at 16 and 32 weeks (Fig. 1B). These results suggest that CD4⁺CD25⁺ T cells promote tumor growth in forestomach tumors.

Increased populations of CD4⁺CD25⁺ T cells in RLNs of B[a]P-induced forestomach tumors in mice

In order to evaluate whether tumor-bearing hosts with forestomach carcinoma have an increased population of Treg cells in the lymphoid organs, the expression of surface molecules on T cells was analyzed by flow cytometry. The RLNs of the B[a]P-treated mice

had a significantly higher proportion of CD4⁺CD25⁺ T cells ($9.26 \pm 1.56\%$; $9.61 \pm 0.52\%$; $5.09 \pm 2.03\%$) compared to corn oil-treated ($3.72 \pm 0.83\%$; $3.07 \pm 1.52\%$; $2.45 \pm 0.70\%$) at 7, 16 and 32 weeks, respectively. The population of CD4⁺CD25⁺ T cells in total CD4⁺ T cells ($13.51 \pm 2.21\%$; $17.63 \pm 2.62\%$; $9.36 \pm 4.75\%$) was also significantly increase when compared with control group ($5.57 \pm 1.79\%$; $5.73 \pm 2.95\%$; $4.51 \pm 1.15\%$)(Fig. 2B).

To assure that the majority of CD25⁺ T cells expressed on the CD4⁺ T cells not the CD8⁺ T cells, CD25 expression on CD8⁺ T cells was assessed. The RLNs of the B[a]P group contained a similar percentage of CD8⁺CD25⁺ or CD8⁺CD25⁺ T cells in total CD8⁺ T cells than those of the control group at 7 and 32 weeks (Fig. 2B). In particular, it was shown that, in the B[a]P-treated mice, there was a significantly higher proportion of CD8⁺CD25⁺ or CD8⁺CD25⁺ T cells in total CD8⁺ T cells in comparison to the corn oil-treated at 16 weeks (Fig. 2B). From the results, we confirmed that the majority of CD25⁺ T cells expressed on the CD4⁺ T cells not the CD8⁺ T cells during B[a]P treatment.

The population of CD4⁺CD25⁺ or CD8⁺CD25⁺ T cells in B[a]P-treated and CD25-depleted mice was also assessed. At 16 weeks, the population of CD4⁺CD25⁺ T cells in total CD4⁺ T cells in the RLNs of the B[a]P/PC61 group was significantly inhibited relative to the B[a]P/IgG group. Further, the population of CD8⁺CD25⁺ T cells in total CD8⁺ T cells in the RLNs of the B[a]P/PC61 was significantly inhibited compared with the B[a]P/IgG group at 16 and 32 weeks (Fig. 2B).

Distribution of CD4⁺CD25⁺ T cell populations in PLNs, spleen and thymus of

B[a]P-induced forestomach tumors in mice

To clarify the induction of Treg cells from different lymphoid tissues in forestomach carcinoma, the Treg cells of the PLNs were analyzed. The frequency of CD4⁺CD25⁺ and CD4⁺CD25⁺ T cells in total CD4⁺ T cells ($6.42 \pm 0.59\%$ and $10.96 \pm 0.28\%$, respectively) in the PLNs of the B[a]P group were significantly increased when compared with the control

group ($3.50 \pm 1.11\%$; $5.52 \pm 1.78\%$, respectively) at 16 weeks (Fig. 2B). The $CD8^+CD25^+$ and $CD8^+CD25^+$ T cells in total $CD8^+$ cells were also evaluated in the PLNs. The population of $CD8^+CD25^+$ T cells in total $CD8^+$ cells ($13.9 \pm 2.27\%$; $14.6 \pm 0.84\%$) in the PLNs of B[a]P group was significantly increased compared with the control group ($7.64 \pm 1.96\%$; $3.48 \pm 2.21\%$) at 7 and 16 weeks, respectively (Fig. 2B).

After depletion, there was a significant reduction in the frequency of $CD4^+CD25^+$ T cells in total $CD4^+$ cells in the PLNs of the B[a]P/PC61 group at 16 weeks. The population of $CD8^+CD25^+$ T cells in total $CD8^+$ T cells in the PLNs of B[a]P/PC61 group were also significantly reduced at 7 and 16 weeks (Fig. 2B).

Comparing the populations of $CD4^+CD25^+$ T cells in total $CD4^+$ T cells ($8.47 \pm 1.21\%$; $8.86 \pm 1.15\%$) of the spleens, the B[a]P group was significantly increased compared with the control group ($5.48 \pm 0.99\%$; $4.52 \pm 1.16\%$) at 7 and 32 weeks (Fig. 2C). The frequency of $CD8^+CD25^+$ T cells in total $CD8^+$ T cells ($12.99 \pm 1.87\%$) of the spleens for the B[a]P group was significantly increased compared with the control group ($3.74 \pm 1.40\%$) at 32 weeks (Fig. 2C). After further comparing the difference among B[a]P/IgG, B[a]P/PC61 and control groups, the frequency of $CD4^+CD25^+$ T cells in total $CD4^+$ T cells and $CD8^+CD25^+$ T cells in total $CD8^+$ T cells of the spleen for the B[a]P/PC61 group was significantly reduced at 32 weeks (Fig. 2C). There exists similar distributions of $CD4^+CD25^+$, $CD8^+CD25^+$, $CD4^+$ and $CD8^+$ T cells in the lymphocytes of the thymus. The populations of $CD4^+$ and $CD8^+$ T cells of RLNs, PLNs, spleen and thymus were consistent in B[a]P-treated and B[a]P-treated/CD25-depleted mice at 7, 16 and 32 weeks (data not shown). The $CD3^+$ T cells in RLNs, PLNs and spleen by flow cytometry at various time points revealed that the pattern of surface expression for CD3 in the RLNs, PLNs and spleen were similar comparing the control, B[a]P/IgG and B[a]P/PC61 groups at 7, 16 and 32 weeks (data not shown). Taken together, these results reveal that the proportion of $CD4^+CD25^+$ T cells is clearly increased in RLNs compared with PLNs, thymus and spleen in the B[a]P group.

Depletion of CD25⁺ T cells enhances apoptosis in tumor nodules in forestomach cancer

We investigated whether depletion of CD25⁺ cells could increase the antitumor effect of host. In fact, massive apoptotic cells observed in the forestomach squamous cell carcinomas of B[a]P-treated and CD25-depleted mice compared to their B[a]P/IgG-treated mice at 16 and 32 weeks (Fig. 3). Further, apoptosis occurred frequently in the forestomach tumor nodules of B[a]P-treated and CD25-depleted mice at 32 weeks (Fig. 3).

CD4⁺CD25⁺ T cells of RLNs and PLNs express the Foxp3 transcription factor

Foxp3 is a crucial transcription factor and the specific marker for regulatory T cells. Flow sorting was used for enumeration of isolated CD4⁺CD25⁺ (combined CD25^{int} and CD25^{high}-expressing cells) and CD4⁺CD25⁻ T cells within RLNs, PLNs or thymus (Fig. 4A). We tested the expression of Foxp3 in CD4⁺CD25⁺ and CD4⁺CD25⁻ cells in the RLNs and PLNs of the B[a]P and control groups at various time points using RT-PCR and real-time PCR.

As expected, CD4⁺CD25⁺ T cells of the RLNs and PLNs expressed high levels of Foxp3, while CD4⁺CD25⁻ T cells of the RLNs and PLNs expressed only low levels in the B[a]P group (Fig. 4B, C, D). Further, the Foxp3 transcripts of CD4⁺CD25⁺ T cells were dramatically enhanced in RLNs relative to PLNs at 32 weeks (Fig. 4D).

We further analyzed whether the CD4⁺CD25⁺ or CD4⁺CD25⁻ T cells of the RLNs and PLNs produce immunosuppressive cytokines such as IL10 and TGF-β1. Results revealed that the two types of T cells of the RLNs and PLNs in the B[a]P-treated mice enhanced expression of IL10 at transcription levels at 32 weeks (Fig. 4B, C). In control mice, only the CD4⁺CD25⁺ T cells of the RLNs express the low level IL-10 transcripts at 32 weeks. We found that the CD4⁺CD25⁺ and CD4⁺CD25⁻ T cells of the RLNs and PLNs in B[a]P-treated and control mice produce little or no IL10 transcripts at 7 and 16 weeks (data not shown). We also examined the expression patterns of TGF-β1 in the CD4⁺CD25⁺ T cells and CD4⁺CD25⁻

T cells of the RLNs and PLNs in the B[a]P-treated and control mice. These were negative for the TGF- β 1 transcripts at 7, 16 and 32 weeks. In PLNs, only the CD4⁺CD25⁻ T cells from the B[a]P-treated mice produce low levels of the TGF- β 1 transcripts at 32 weeks (Fig. 4B, C). These findings suggest that Foxp3 expression of CD4⁺CD25⁺ T cells demonstrated the activation of Treg cells and associated with the effect of CD4⁺CD25⁺ T cells for tumor formation. Moreover, production of IL-10 not TGF- β 1 transcripts has been implicated as a mediator of inhibition for immune functions during tumor progression.

Increased populations of CD4⁺CD25⁺ T cells in total CD4⁺ cells in PBMC and N1 regional lymph nodes with human gastric cancers

In order to confirm the increased prevalence of CD4⁺CD25⁺ T cells in peripheral blood mononuclear cells (PBMC) and N1 regional lymph nodes from patients with advanced gastric cancer, the CD4⁺ and CD4⁺CD25⁺ T cells of PBMC, normal mucosa, tumor, and N1 lymph nodes were examined. Results reveal that the frequency of CD4⁺CD25⁺ T cells in total CD4⁺ T cells in PBMC, tumor, and N1 regional lymph nodes was significantly higher in gastric cancer patients than in healthy donors (PBMC: 8.29 ± 1.73 %, n=7), those in the tumor and N1 lymph node were also significantly increase in advanced gastric cancer than in early gastric cancer (Table 2). There is an increased trend of Treg cells observed in PBMC, tumor, and N1 regional lymph nodes during disease progression. These findings suggest that the increased population of Treg cells in the N1 regional lymph nodes may be one of the actions for associated the immune dysfunction of host for tumor progressive in gastric cancer.

Discussion

Gastric cancer is one of the most common cancers in the world, and lymph node metastasis is the most determinative for patient survival. There are many submucosal associated lymphoid tissues responsible for the immunoserveillance in the gastrointestinal

tract. One of the important roles of the immune system is combating cancer cells, which reduce or inhibit the development and progression of tumors. But Treg cells may dampen host antitumor response via immunosuppressive effect. An increase of Treg cells was shown correlated with immunosuppression and tumor progression in patients with gastrointestinal cancers (6). So far, there is no evidence to address the changes of Treg cells of lymph nodes at initiation stage of gastric cancer development in human or animals. In this study, we clearly demonstrate that the proportion of Treg cells increase in the lymphoid tissues during the tumor progression, especially in the regional lymph nodes, in benzo[a]pyrene-induced mouse forestomach carcinoma. These Treg cells from regional lymph nodes and peripheral nodes are induced by tumor and both significantly display enhanced levels of Foxp3 mRNA expression. The Treg cells were depleted by anti-CD25 mAb (PC61) after 5 weeks of B[a]P treatment, significant decrease of Treg cells in the RLNs, reduction of forestomach tumor nodules development along with massive apoptosis cells were found in the tumor nodules.

Despite efforts for treatment of cancer, a large number of tumors continue to grow and evade recognition and/or destruction by the immune system. It is believed that a T-cell response does exist but is ineffective. Treg cells are known to be immunoregulatory and are important in immunological tolerance to self-antigens and inhibition of T-cell proliferation (1-5). These observations provide evidence that Treg cells play role in the immune dysfunction in cancer patients. Therefore, decreasing the Treg cells would be one of the immunotherapies for treating cancer. Suttmuller et al further clearly demonstrated that depletion of Treg cells enhanced T-cells reactivity to a known tumor-associated antigen (24). However, it is thought that only depletion of the Treg cells is not sufficient to treat established cancer. Actually, in most of the relevant research, anti-CD25 mAb (PC61) was administered for depletion of Treg cells several days prior to tumor implantation or only 1 day afterwards (22, 24, 27, 32-35). In our murine model for long term studies, we demonstrated that although the CD25⁺ cells in lymph nodes were not completely inhibited in

mice for tumor progressive process, tumor growth in the forestomach was remarkably reduced. This suggests that the increase in the Treg cells of tumor-draining lymph nodes may have inhibited local immunosuppressive response during tumorigenesis. A consecutive course of depleted-antibody injections, with no histological indication of autoimmune disease observed in the mice 6 months after the antibody treatment, was sufficient to cause regression of the tumors.

It is important to note that activation of Treg cells in RLNs may control tumor-associated antigen specific immunity during the course of forestomach cancer development. Tanaka and coworkers (27) have demonstrated the immune enhancing effects of depletion of Treg cells on the sensitization of T cells in tumor-draining lymph node for adoptive immunotherapy. In accordance with previous studies, depletion of Treg cells increases the generation of specific immune T cells (22, 27). Depletion of CD25⁺ T cells facilitates infiltration of CD8⁺ T cells at tumor sites, so the Treg cells probably the main subset of CD4⁺ T cells responsible for the observed enhancement (36). These studies suggest that removal of Treg cells leads to generation of tumor-specific CD8 T cells and tumor-nonspecific CD4⁻CD8⁻ effector cells *in vivo*. In this study, we also observed massive cell infiltration at the tumor sites, and apoptosis in the tumor mass in B[a]P-treated/CD25-depleted mice at 32 weeks. Therefore, removal of CD25⁺ T cells may evoke effective immune responses via enhancement of the development of tumor-specific CD4⁺CD25⁻ and CD8⁺CD25⁻ T cells or others, such as granulocytes. That is to say, the existence of Treg cells in RLN attenuates granulocyte infiltration in the tumor mass, and that Treg cells inhibit not only specific T cell infiltration, but also innate immune responses such as granulocyte infiltration. Previous studies have described how Treg cells inhibit innate immune activation through cytokine-dependent mechanisms (37). Moreover, granulocyte-mediated tumor-cell apoptosis plays an important role in tumorigenicity (31, 38). The important role of neutrophils in antitumor immunity has been demonstrated in depletion experiments using specific mAb for neutrophils in a murine melanoma model (38). Therefore,

we suggested that the effect of Treg cells in the RLNs also inhibit innate immunity in forestomach carcinoma. Interestingly, we cultured isolated murine tumor cells from forestomach cancers *in vitro*, using RT-PCR for to determine the levels of IL-10, TGF- β 1 and Fas/FasL mRNA analysis of these tumor cells, which expressed mRNA for Fas and TGF- β 1, but not for FasL and IL-10 (unpublished data). The production of immunosuppressive factors by tumors or the induction of such factors by tumor-infiltrating cells may contribute to evasion of immune attack. Therefore, our results implicate that tumor destruction may be caused by neutrophil-mediated killing through Fas/ FasL-mediated cytotoxicity pathway. However, this postulate still needs to be demonstrated.

FoxP3, one surface molecule on Treg cells, plays a vital role in the development of CD25⁺ Treg cells and displays a unique functional significance (27). And these Treg cells can produce suppressor cytokines such as IL-10 or TGF- β 1. In this study, we demonstrated the strong Foxp3 transcript induction of Treg cells has been observed in RLN and PLN in late-stage cancer. In particular, the increased Foxp3 transcript of Treg cells in RLNs was significantly higher than that in PLNs. Further, the IL-10 transcript of CD4⁺CD25⁺ and CD4⁺CD25⁻ T cells in the RLNs and PLNs were induced in late-stage forestomach cancer. These results suggest that IL-10-mediated suppression of activated Treg cells confers the ability to adapt to tumor immunity. One critical question that remains to be addressed is which factors are capable of contributing to Treg cell proliferation, expansion and activation in RLN.

In advanced-stage cancer, increased prevalence of peripheral-blood Treg cells has been reported in patients with lung, pancreas, breast, stomach and ovarian cancers (8, 9, 11, 13, 15). More noteworthy is that in our investigation of B[a]P-induced forestomach cancers in mice, we demonstrated that the population of Treg cells was increased in the RLNs, PLNs and spleen, but not the thymus. Nonetheless, in our study we found that CD4⁺CD25⁺ T cells were more abundant in local regional lymph nodes compared to other lymphoid tissues in

forestomach cancer. Further, consistent with results from patients with gastric cancer, the frequency of Treg cells increased in N1 regional lymph nodes in advanced gastric cancers. Previous studies have indicated that Treg cells suppress the T cell priming that often occurs in lymph nodes (2, 39, 40). In forestomach cancer, the Treg cells of the RLNs were strongly associated with progressive tumor growth. Analysis of our data reveals overrepresentation of Treg cells and expression of high levels of Foxp3 in RLNs, suggesting that they may play a suppressive role in local immune responses. These accumulated Treg cells may also inhibit effector cell functions in late tumor stages.

The enhancement of CD4⁺CD25⁺ T cells of local regional lymph nodes may be the cause of immunity tolerance. In this study, the most significant finding is the increased population of Treg cells in regional lymph nodes associated with progressive forestomach carcinomas, inhibiting activation and expansion of Treg cells can evoke effective local immunity. That is to say, the accumulation of Treg cells in RLNs mediated harmful local immune responses in progressive forestomach tumor. Removal of Treg cells of tumor-draining lymph nodes can evoke local response to prevent progression of tumor. Chemoprevention is an approach to reduce the occurrence of cancer and deals with the chemotherapy of preinvasive neoplasia, dysplasia, or intraepithelial neoplasia, depending on the organ system (41). Based on our results, we suggest the use of antibodies or fusion proteins to reduce or eliminate human suppression cells in the local site and combine the use of drugs in the chemoprevention to gain maximal benefit during treatment of gastric cancer.

Acknowledgements

This study was supported by Grant NSC93-2320-B41-010 and NSC93-2314-B-006-112 from the National Science Council, Taiwan.

References

1. Maloy KJ, Powrie F. Regulatory T cells in the control of immune pathology. *Nat Immunol* 2001; 2: 816-22.
2. Sakaguchi S, Sakaguchi N, Shimizu J, et al. Immunologic tolerance maintained by CD25⁺ CD4⁺ regulatory T cells: their common role in controlling autoimmunity, tumor immunity, and transplantation tolerance. *Immunol Rev* 2001; 182: 18-32.
3. Gavin M, Rudensky A. Control of immune homeostasis by naturally arising regulatory CD4⁺ T cells. *Curr Opin Immunol* 2003; 15: 690-6.
4. Piccirillo CA, Shevach EM. Naturally-occurring CD4⁺CD25⁺ immunoregulatory T cells: central players in the arena of peripheral tolerance. *Semin Immunol* 2004; 16: 81-8.
5. Piccirillo CA, Thornton AM. Cornerstone of peripheral tolerance: naturally occurring CD4⁺CD25⁺ regulatory T cells. *Trends Immunol* 2004; 25: 374-80.
6. Sasada T, Kimura M, Yoshida Y, Kanai M, Takabayashi A. CD4⁺CD25⁺ regulatory T cells in patients with gastrointestinal malignancies: possible involvement of regulatory T cells in disease progression. *Cancer* 2003; 98: 1089-99.
7. Kawaida H, Kono K, Takahashi A, et al. Distribution of CD4⁺CD25^{high} regulatory T-cells in tumor-draining lymph nodes in patients with gastric cancer. *J Surg Res* 2005; 124: 151-7.
8. Ichihara F, Kono K, Takahashi A, Kawaida H, Sugai H, Fujii H. Increased populations of regulatory T cells in peripheral blood and tumor-infiltrating lymphocytes in patients with gastric and esophageal cancers. *Clin Cancer Res* 2003; 9: 4404-8.
9. Wolf AM, Wolf D, Steurer M, Gastl G, Gunsilius E, Grubeck-Loebenstien B. Increase of regulatory T cells in the peripheral blood of cancer patients. *Clin Cancer Res* 2003; 9: 606-12.
10. Curiel TJ, Coukos G, Zou L, et al. Specific recruitment of regulatory T cells in ovarian carcinoma fosters immune privilege and predicts reduced survival. *Nat Med* 2004; 10:

942-9.

11. Woo EY, Chu CS, Goletz TJ, et al. Regulatory CD4(+)CD25(+) T cells in tumors from patients with early-stage non-small cell lung cancer and late-stage ovarian cancer. *Cancer Res* 2001; 61: 4766-72.
12. Ormandy LA, Hillemann T, Wedemeyer H, Manns MP, Greten TF, Korangy F. Increased populations of regulatory T cells in peripheral blood of patients with hepatocellular carcinoma. *Cancer Res* 2005; 65: 2457-64.
13. Liyanage UK, Moore TT, Joo HG, et al. Prevalence of regulatory T cells is increased in peripheral blood and tumor microenvironment of patients with pancreas or breast adenocarcinoma. *J Immunol* 2002; 169: 2756-61.
14. Woo EY, Yeh H, Chu CS, et al. Cutting edge: Regulatory T cells from lung cancer patients directly inhibit autologous T cell proliferation. *J Immunol* 2002; 168: 4272-6.
15. Viguiere M, Lemaitre F, Verola O, et al. Foxp3 expressing CD4⁺CD25(high) regulatory T cells are overrepresented in human metastatic melanoma lymph nodes and inhibit the function of infiltrating T cells. *J Immunol* 2004; 173:1444-53.
16. Phillips DH. Polycyclic aromatic hydrocarbons in the diet. *Mutat Res* 1999; 443: 139-47.
17. Halliwell B, Gutteridge JM. *Free Radicals in Biology and Medicine*, second ed. New York Oxford University, Clarendon Press, USA; 1989. pp. 466-95.
18. Deshpande SS, Ingle AD, Maru GB. Inhibitory effects of curcumin-free aqueous turmeric extract on benzo[a]pyrene-induced forestomach papillomas in mice. *Cancer Lett* 1997; 16, 79-85.
19. Agha AM, El-Fattah AA, Al-Zuhair HH, Al-Rikabi AC. Chemopreventive effect of Ginkgo biloba extract against benzo(a)pyrene-induced forestomach carcinogenesis in mice: amelioration of doxorubicin cardiotoxicity. *J Exp Clin Cancer Res* 2001; 20, 39-50.
20. Fahey JW, Haristoy X, Dolan PM, et al. Sulforaphane inhibits extracellular, intracellular, and antibiotic-resistant strains of *Helicobacter pylori* and prevents

- benzo[a]pyrene-induced stomach tumors. *Proc Natl Acad Sci USA* 2002; 99:7610-5.
21. Goswami UC, Sharma N. Efficiency of a few retinoids and carotenoids in vivo in controlling benzo[a]pyrene-induced forestomach tumour in female Swiss mice. *Br J Nutr* 2005; 94:540-3.
 22. Shimizu J, Yamazaki S, Sakaguchi S. Induction of tumor immunity by removing CD25⁺CD4⁺ T cells: a common basis between tumor immunity and autoimmunity. *J Immunol* 1999; 163: 5211-8.
 23. Onizuka S, Tawara I, Shimizu J, Sakaguchi S, Fujita T, Nakayama E. Tumor rejection by in vivo administration of anti-CD25 (interleukin-2 receptor alpha) monoclonal antibody. *Cancer Res* 1999; 59: 3128-33.
 24. Suttmuller RP, van Duivenvoorde LM, van Elsas A, et al. Synergism of cytotoxic T lymphocyte-associated antigen 4 blockade and depletion of CD25(+) regulatory T cells in antitumor therapy reveals alternative pathways for suppression of autoreactive cytotoxic T lymphocyte responses. *J Exp Med* 2001; 194: 823-32.
 25. Wattenberg LW, Lam LK, Fladmoe AV. Inhibition of chemical carcinogen-induced neoplasia by coumarins and alpha-angelicalactone. *Cancer Res.* 1979; 39: 1651-4.
 26. Wu K, Shan YJ, Zhao Y, Yu JW, Liu BH. Inhibitory effects of RRR-alpha-tocopheryl succinate on benzo(a)pyrene (B(a)P)-induced forestomach carcinogenesis in female mice. *World J Gastroenterol* 2001; 7: 60-5.
 27. Tanaka H, Tanaka J, Kjaergaard J, Shu S. Depletion of CD4⁺ CD25⁺ regulatory cells augments the generation of specific immune T cells in tumor-draining lymph nodes. *J Immunother* 2002; 25: 207-17.
 28. Hori S, Nomura T, Sakaguchi S. Control of regulatory T cell development by the transcription factor Foxp3. *Science* 2003; 299: 1057-61.
 29. Shull MM, Ormsby I, Kier AB, et al. Targeted disruption of the mouse transforming growth factor-beta 1 gene results in multifocal inflammatory disease. *Nature* 1992; 359:

- 693-9.
30. Matsuura M, Okazaki K, Nishio A, et al. Therapeutic effects of rectal administration of basic fibroblast growth factor on experimental murine colitis. *Gastroenterology* 2005; 128: 975-86.
 31. Chen YL, Wang JY, Chen SH, Yang BC. Granulocytes mediates the Fas-L-associated apoptosis during lung metastasis of melanoma that determines the metastatic behaviour. *Br J Cancer* 2002; 87: 359-65.
 32. Li J, Hu P, Khawli LA, Epstein AL. Complete regression of experimental solid tumors by combination LEC/chTNT-3 immunotherapy and CD25(+) T-cell depletion. *Cancer Res* 2003; 63: 8384-92.
 33. Tawara I, Take Y, Uenaka A, Noguchi Y, Nakayama E. Sequential involvement of two distinct CD4⁺ regulatory T cells during the course of transplantable tumor growth and protection from 3-methylcholanthrene-induced tumorigenesis by CD25-depletion. *Jpn J Cancer Res* 2002; 93: 911-6.
 34. Jones E, Dahm-Vicker M, Simon AK, et al. Depletion of CD25⁺ regulatory cells results in suppression of melanoma growth and induction of autoreactivity in mice. *Cancer Immun* 2002; 2: 1.
 35. Casares N, Arribillaga L, Sarobe P, et al. CD4⁺/CD25⁺ regulatory cells inhibit activation of tumor-primed CD4⁺ T cells with IFN-gamma-dependent antiangiogenic activity, as well as long-lasting tumor immunity elicited by peptide vaccination. *J Immunol* 2003; 171: 5931-9.
 36. Lin CC, Chou CW, Shiau AL, et al. Therapeutic HER2/Neu DNA vaccine inhibits mouse tumor naturally overexpressing endogenous neu. *Mol Ther* 2004; 10: 290-301.
 37. Maloy KJ, Salaun L, Cahill R, Dougan G, Saunders NJ, Powrie F. CD4⁺CD25⁺ T(R) cells suppress innate immune pathology through cytokine-dependent mechanisms. *J Exp Med* 2003; 197: 111-9.

38. Chen YL, Chen SH, Wang JY, Yang BC. Fas ligand on tumor cells mediates inactivation of neutrophils. *J Immunol* 2003; 171:1183-91.
39. Shevach EM. CD4⁺ CD25⁺ suppressor T cells: more questions than answers. *Nat Rev Immunol* 2002; 2: 389-400.
40. Von Herrath MG, Harrison LC. Regulatory lymphocytes: antigen-induced regulatory T cells in autoimmunity. *Nat Rev Immunol* 2003; 3: 223-32.
41. Kelloff GJ, Boone CW, Steele VE, Crowell JA, Lubet R, Sigman CC. Progress in cancer chemoprevention: perspectives on agent selection and short-term clinical intervention trials. *Cancer Res* 1994; 1: 2015s-24s.

Figure Legends

Figure 1. Pathological observation of forestomach tumors in mice. **A**, Photomicrography of forestomach tumors in mice. Control mice were treated with corn oil. B[a]P-treated mice were treated with corn oil and benzo[a]pyrene by p.o. gavage twice a week for 4 weeks. Mice were then sacrificed at 16 and 32 weeks after first administration of benzo[a]pyrene. The B[a]P/PC61 mice were injected i.p. with ascetic fluid from PC61 mAb twice a week beginning 5 weeks after B[a]P treatment. The B[a]P/IgG mice received the same treatment with purified rat IgG Ab. **B**, Mice were sacrificed at 16 and 32 weeks and their stomachs excised. Tissues samples were stained with hematoxylin and eosin. The numbers of papilloma and squamous cell carcinomas were both increased in B[a]P/IgG and B[a]P/PC61 mice, but at the tumor sites showed a increase of granulocyte and lymphocyte infiltration in B[a]P/PC61 mice.

Figure 2. CD4⁺CD25⁺ T cells in distinct microenvironments. **A**, CD4⁺CD25⁺ T cells of lymphoid tissues were reduced in naïve mice with PC61 mAb-treated. Axillaries, inguinal, brachial, and popliteal lymph nodes were also collected and defined as peripheral lymph nodes (PLNs). The percentage of CD4⁺CD25⁺ T cells in PLNs, spleen and thymus in rat IgG

or PC61 Ab-treated naïve mice. Flow cytometry analyses after the depletion of CD25⁺ T cells in the naïve mice revealed populations under 1% in PLNs, spleen and thymus. **B**, Increased CD4⁺CD25⁺ T cells of RLNs in B[a]P/IgG group. Flow data analysis of the percentages of CD4⁺CD25⁺, CD4⁺, CD8⁺CD25⁺, and CD8⁺T cells of RLNs and PLNs in the control, B[a]P/IgG and B[a]P/PC61 groups at 7, 16 and 32 weeks. **C**, Representative flow cytometric analysis of spleen and thymus CD4⁺CD25⁺ T cells in the control, B[a]P/IgG and B[a]P/PC61 groups at 7, 16 and 32 weeks. RLNs, PLNs, spleen and thymus from the mice were collected on weeks 7, 16 and 32 after the first administration of B[a]P. Cell suspensions from the RLNs, PLNs, spleen and thymus were isolated after sterile dissociation, filtration and washing. Lymphocytes of RLNs, PLNs, spleen and thymus were double-stained with FITC-anti-CD25 and PE-anti-CD4 mAbs and assayed using flow cytometry.

Figure 3. Apoptotic cells in forestomach tumors. Apoptotic cells were detected by TUNEL-staining as described in Materials and Methods. Apoptotic cells were revealed by brown color.

Figure 4. CD4⁺CD25⁺ T cells express high level of Foxp3 transcripts. **(A)** RLNs and PLNs CD4⁺CD25⁻ (P2) and CD4⁺CD25⁺ (P3) T cells were sorted and stained with FITC-anti-CD25 and PE-anti-CD4 mAbs. Foxp3, IL-10, TGF-β1 and β-actin mRNA expression of CD4⁺CD25⁺ and CD4⁺CD25⁻ cells in RLNs **(B)** and PLNs **(C)** in B[a]P and control groups at 32 weeks using RT-PCR. Lane 1 and 2: B[a]P group. Lane 3 and 4: control group. Lane 1 and 3: CD4⁺CD25⁻ cells. Lane 2 and 4: CD4⁺CD25⁺ cells. **(D)** Relative Foxp3 expression from CD4⁺CD25⁻ and CD4⁺CD25⁺ T cells using real-time quantitative PCR is shown after normalization to HPRT expression.

Table 1. Depletion of CD25⁺ regulatory cells suppresses forestomach tumor growth

Group	Body wt./mouse (g)	Stomach wt./mouse	% of mice with tumors	Tumors/mouse	Tumor vol. (mm ³)/tumor	Total tumor vol. (mm ³)/mouse
16 wks						
Control	34.7 ± 3.1	0.300 ± 0.020	0	0	0	0
B[a]P/IgG ^{a)}	34.1 ± 2.9	0.343 ± 0.021	100	5.3 ± 1.2 (6, 4, 6)	2.8 ± 0.5 (3.38, 2.67, 2.37)	15 ± 5 (20.29, 10.67, 14.2)
B[a]P/PC61 ^{a)}	33.5 ± 2.7	0.302 ± 0.028	100	3.7 ± 1.5 (5, 4, 2)	0.8 ± 0.5 ^b (0.52, 1.44, 0.52)	3 ± 2 ^b (2.62, 5.76, 1.05)
32 wks						
Control	36.0 ± 4.5	0.352 ± 0.026	0	0	0	0
B[a]P/IgG	36.0 ± 2.5	0.525 ± 0.121 ^b	100	15.5 ± 4.2 (20, 15, 10, 17)	21.1 ± 16.4 (6.0, 16.5, 44.5, 17.5)	276.8 ± 134.5 (119, 247, 444, 297)
B[a]P/PC61	39.7 ± 8.5	0.443 ± 0.030 ^b	100	8.3 ± 2.2 ^b (11, 7, 6, 9)	6.8 ± 3.2 (5.3, 4.9, 5.3, 11.6)	57.1 ± 33.6 ^b (58, 34, 32, 104)

a) Mice were treated with rat IgG or anti-CD25 (PC61) mAb for twice a week beginning 5 weeks after benzo[a] pyrene treatment.

b) P<0.05 compared to B[a]P/IgG.

Table 2. The distribution of Treg cells in different tissues of gastric carcinoma patients

Stage of gastric cancer	Normal mucosa (%)	Tumor (%)	N1 LN (%)	PBMC (%)
Gastric cancer (n=80)	4± 1	25± 4	16± 2	24± 3
Early cancer (n=19)	3± 1	11± 3	10± 2	22± 4
Advanced cancer (n=61)	4± 1	28± 4	17± 2	25± 3

%. The population of CD4⁺CD25⁺ in total CD4⁺ cells.

PBMC of healthy donor: 8.29 ± 1.73%, n=7.

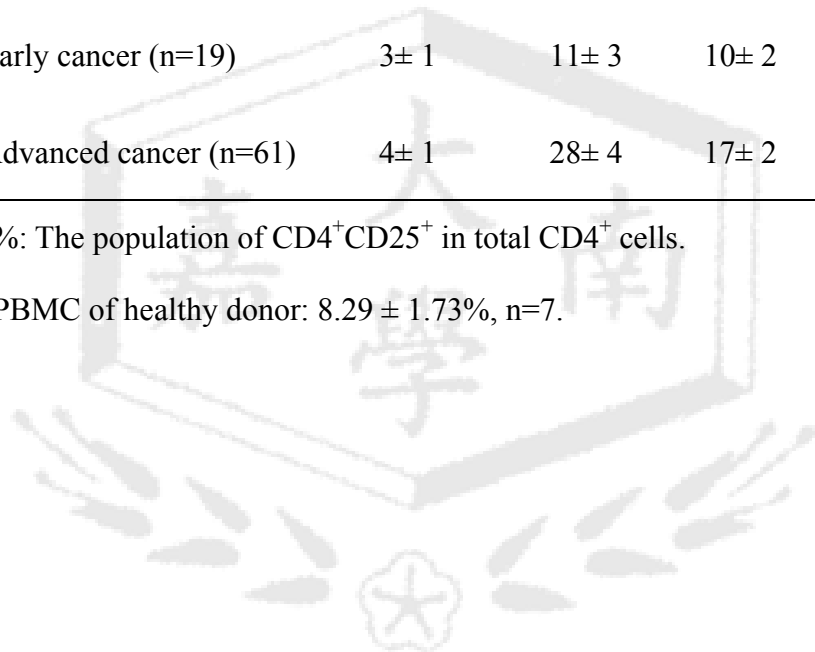


Fig. 1. A

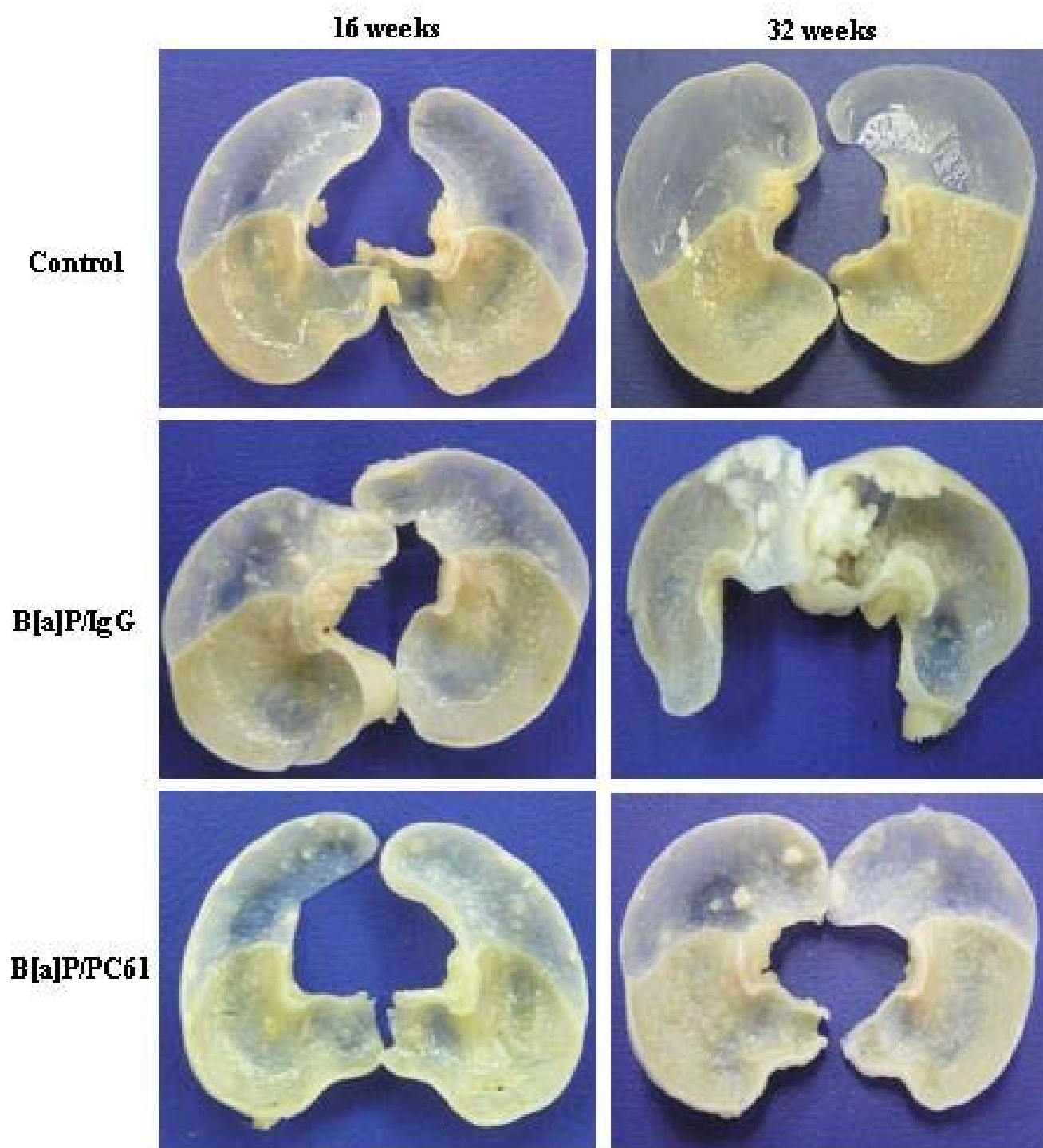
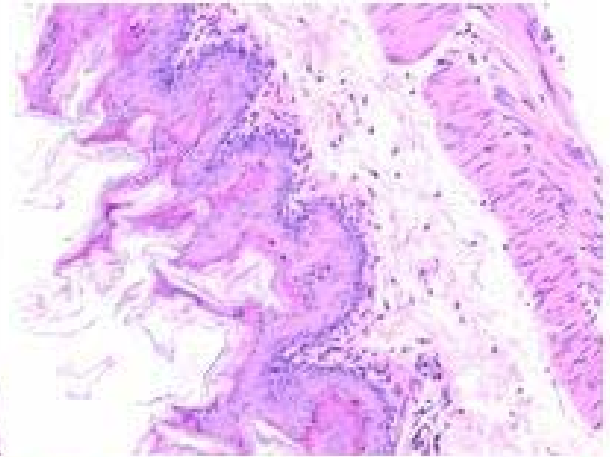
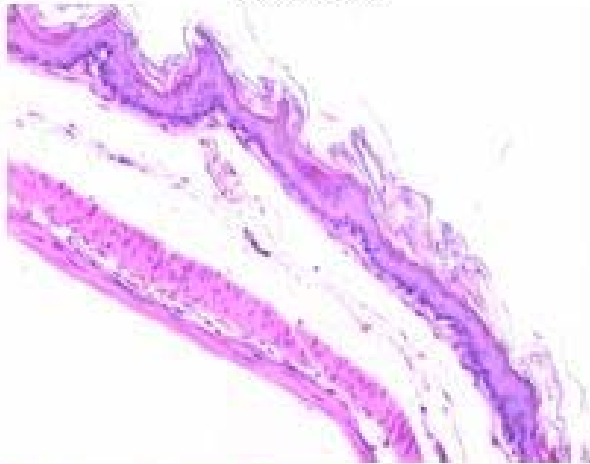


Fig. 1. B

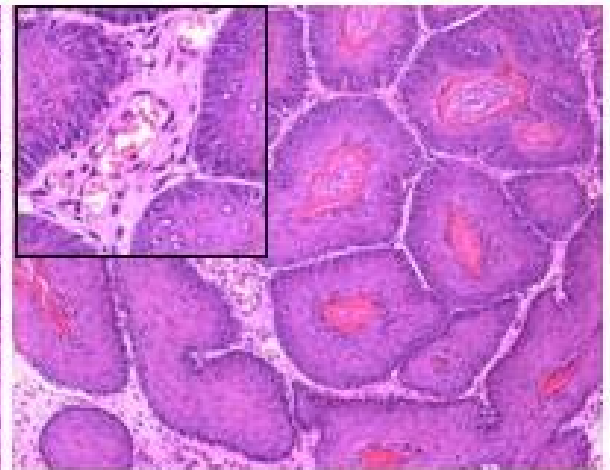
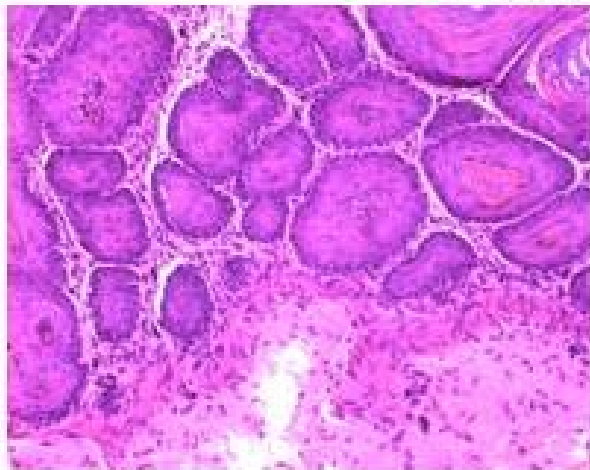
16 weeks

32 weeks

Control



B[a]P/IgG



B[a]P/PC61

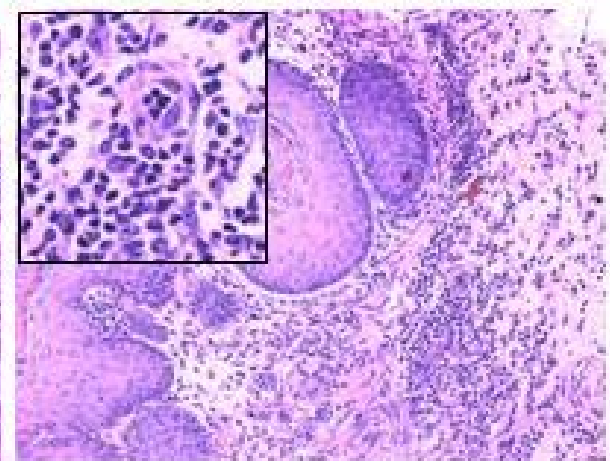
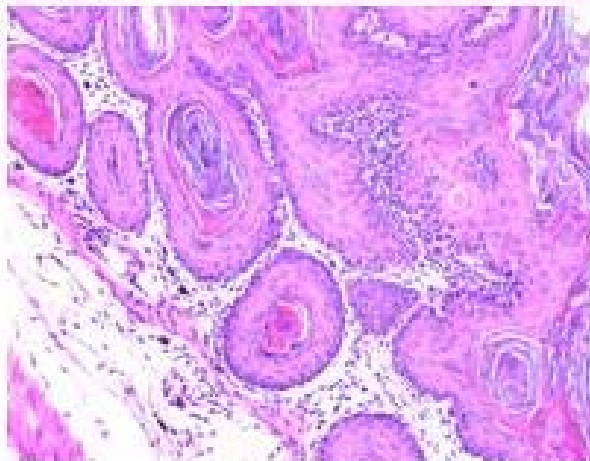


Fig. 2. A

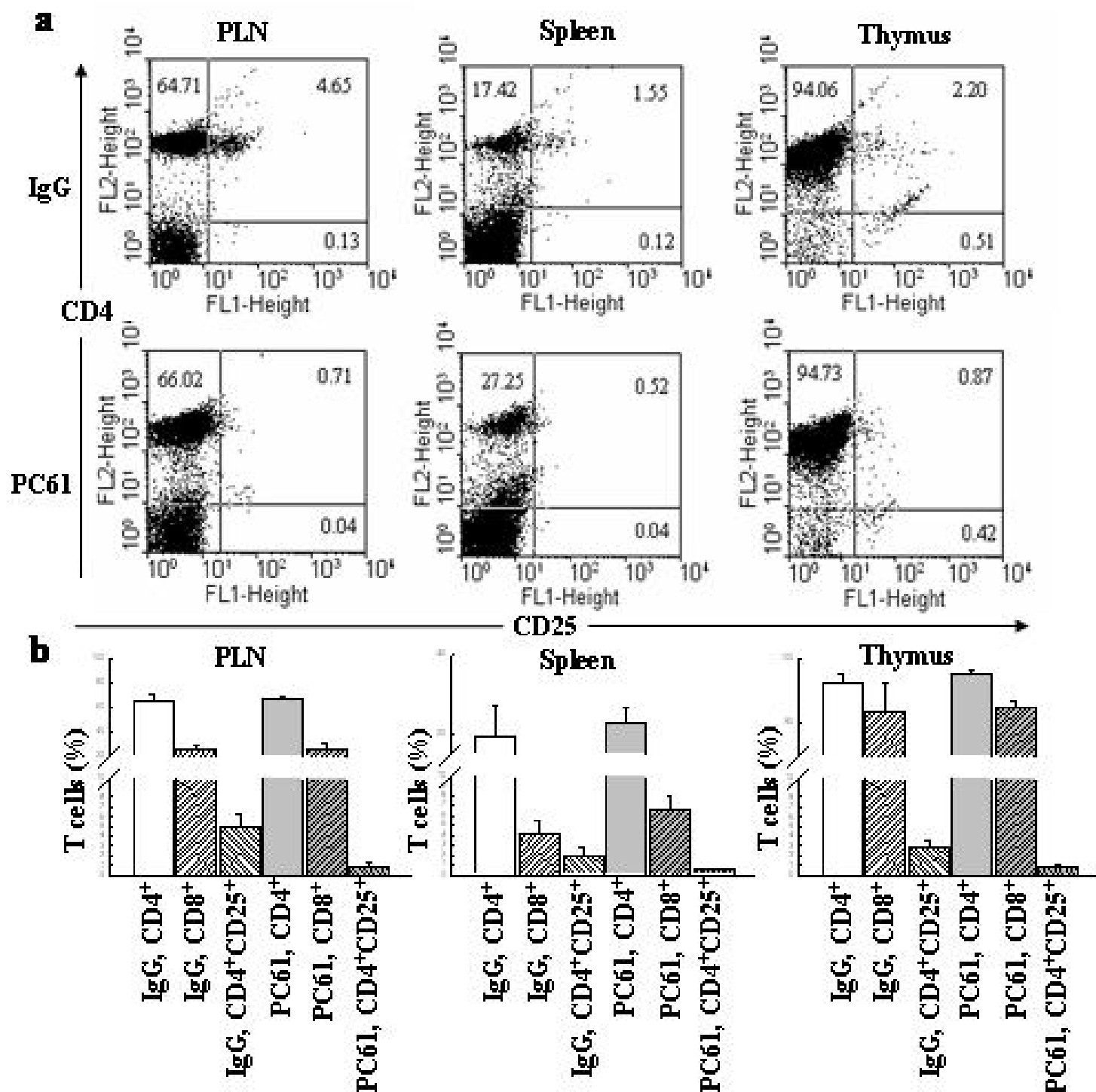


Fig. 2. B

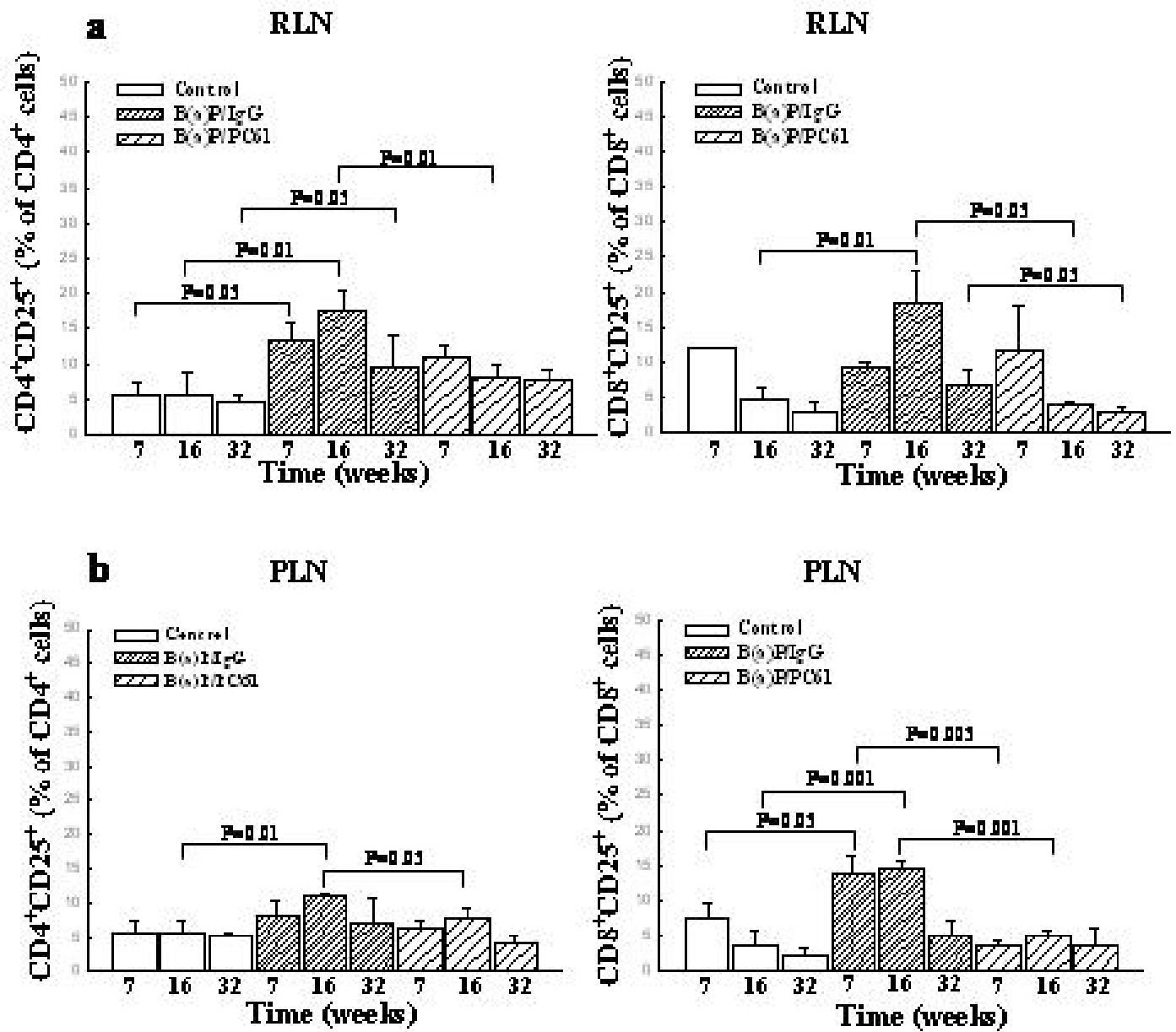


Fig. 2. C

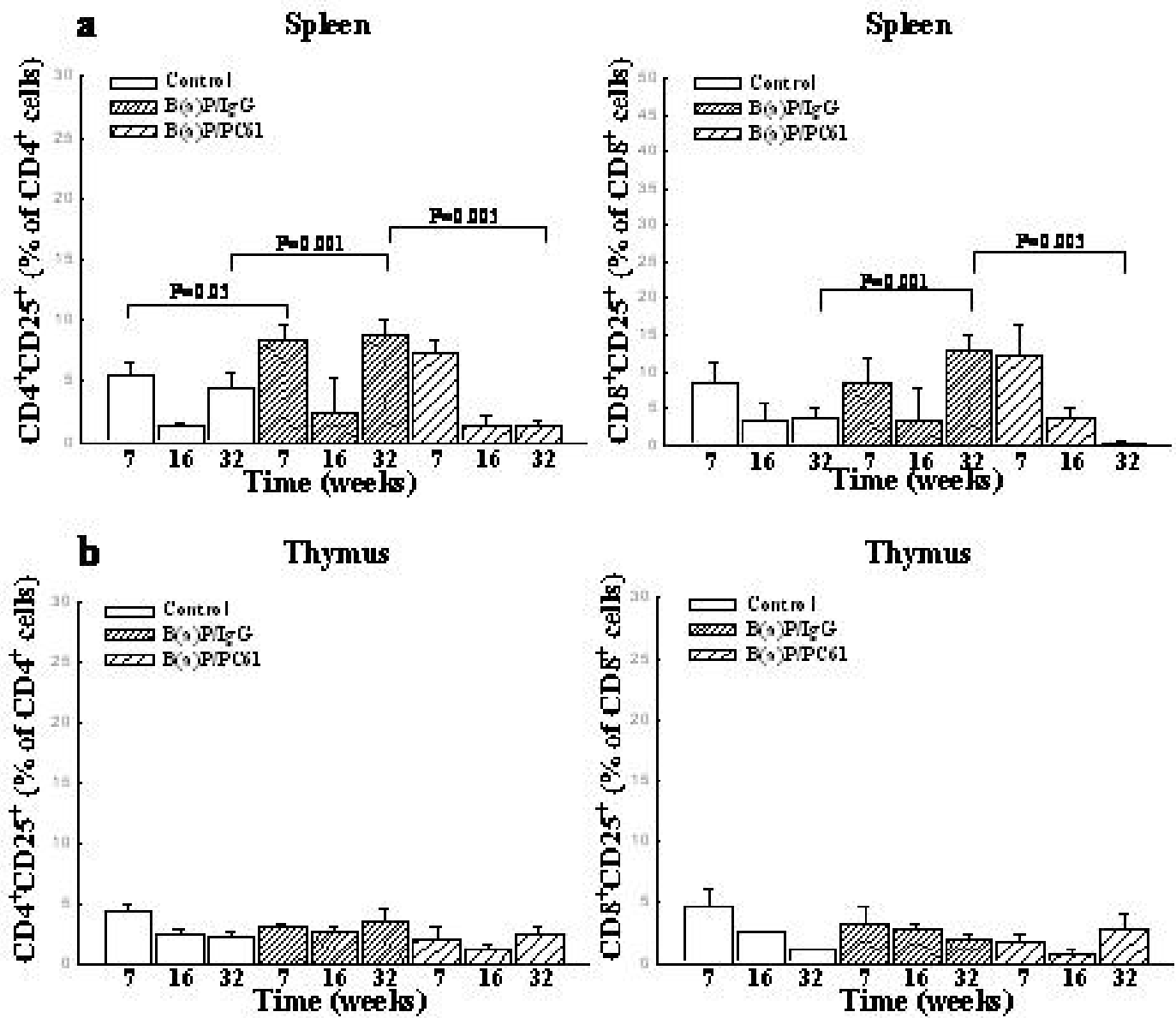


Fig. 3.

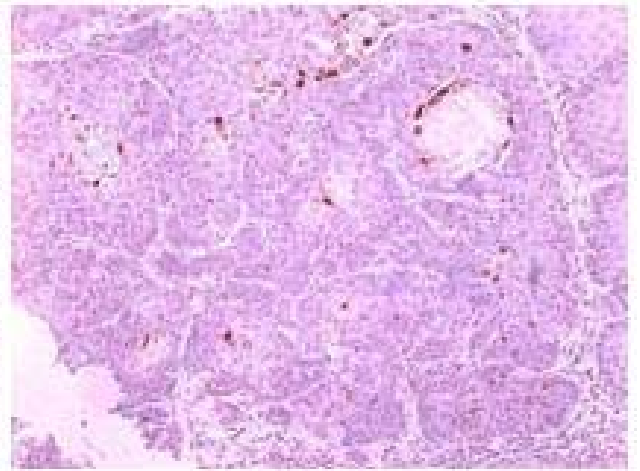
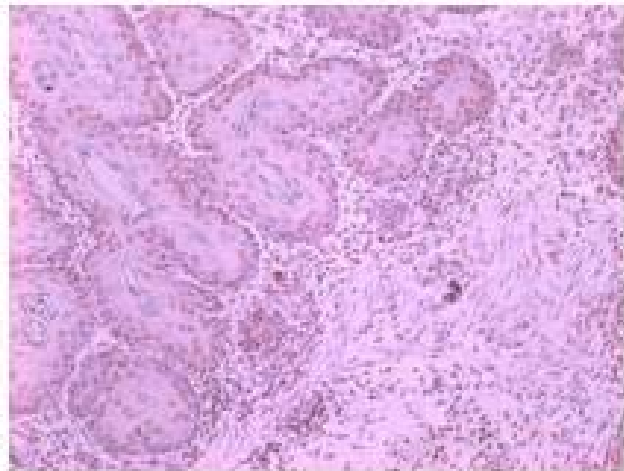
16 weeks

32 weeks

Control



B[a]P/IgG



B[a]P/PC61

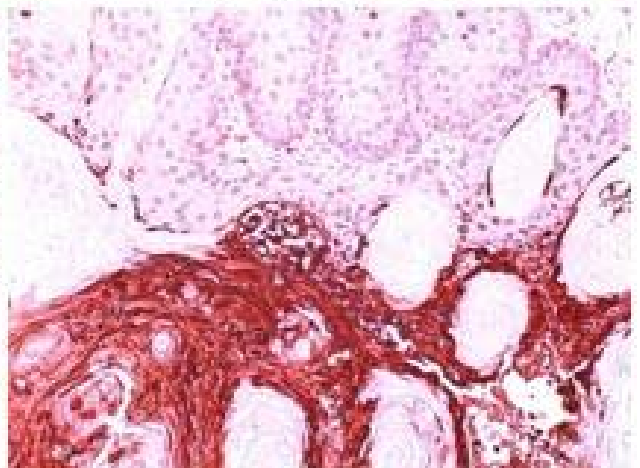


Fig. 4.

